RETROINTEXT: A MULTIMODAL LARGE LANGUAGE MODEL ENHANCED FRAMEWORK FOR RETROSYNTHETIC PLANNING VIA IN-CONTEXT REPRESENTATION LEARNING

Anonymous authors
Paper under double-blind review

ABSTRACT

Development of robust and effective strategies for retrosynthetic planning requires a deep understanding of the synthesis process. A critical step in achieving this goal is accurately identifying synthetic intermediates. Current machine learning-based methods often overlook the valuable context from the overall route, focusing only on predicting reactants from the product, requiring cost annotations for every reaction step, and ignoring the multi-faced nature of molecular, resulting in inaccurate synthetic route predictions. Therefore, we introduce RetroInText, an advanced end-to-end framework based on a multimodal Large Language Model (LLM), featuring in-context learning with TEXT descriptions of synthetic routes. First, RetroInText including ChatGPT presents detailed descriptions of the reaction procedure. It learns the distinct compound representations in parallel with corresponding molecule encoders to extract multi-modal representations including 3D features. Subsequently, we propose an attention-based mechanism that offers a fusion module to complement these multi-modal representations with in-context learning and a fine-tuned LLM for a single-step model. As a result, RetroInText accurately represents and effectively captures the complex relationship between molecules and the synthetic route. In experiments on the USPTO pathways dataset RetroBench, RetroInText outperformed state-of-the-art methods, achieving up to a 5% improvement in Top-1 test accuracy, particularly for long synthetic routes. These results demonstrate the superiority of RetroInText by integrating with context information over routes. They also demonstrate its potential for advancing pathway design and facilitating the development of organic chemistry.

1 INTRODUCTION

Multi-step retrosynthesis planning is a fundamental strategy in organic chemistry, crucial for drug discovery and chemical biology, as it systematically breaks down complex target molecules into simpler, easily accessible precursors (Zheng et al., 2022; Zhong et al., 2023). Recent advancements in deep learning have facilitated the development of various approaches, which can be categorized as template-based, semi-template-based, and template-free approaches aimed at streamlining this process (Zhong et al., 2023; Obonyo et al., 2023; Chen et al., 2020; Coley et al., 2017). Nevertheless, existing methods primarily rely on graph or SMILES representations, and are often limited in capturing the intricate complexities of chemical structures, thereby constraining their scalability and effectiveness in addressing complex retrosynthetic challenges.

Most of the existing retrosynthetic planning strategies (Tripp et al., 2024; Liu et al., 2024c) conceptualize retrosynthetic planning as a search problem, where the synthetic route is represented as a tree or graph, with molecules as nodes. However, a significant limitation of these approaches lies in their reliance on heuristic search algorithms to determine which nodes (molecules) should be expanded. This dependency often leads to several critical challenges, such as ensuring that the expanded nodes are commercially available compounds, avoiding computational inefficiencies, and maintaining the overall feasibility of the synthetic routes (Liu et al., 2023a). Additionally, due to the complex chemical space, each molecule can exhibit a vast number of potential transformations—up

to 10K (Szymkuć et al., 2016). The depth of the search tree, which corresponds to the route length, often varies between 10 to 20 steps, depending on the complexity of the target molecule (Obonyo et al., 2023). This vast combinatorial space, combined with the scarcity of high-quality, structured data for retrosynthetic tasks, limits current methods' ability to effectively explore and prioritize routes, leading to inefficiencies and sub-optimal solutions.

Inspired by the success of LLM, which trained on extensive text corpora, generating coherent text encompassing a wide range of topics and sentiments (Ying et al., 2021). Liu et al. (Liu et al., 2024d) introduced a text-assisted retrosynthesis prediction method that utilizes pre-trained language models to aid reactant generation. In addition, Bran et al. (M. Bran et al., 2024) proposed ChemCrow, by integrating 17 expert-designed tools, ChemCrow enhances the Large Language Models (LLM) performance in chemistry. However, the current LLM method does not include a route length adjustment to guide future searches (Liu et al., 2023a). Despite these advancements, current LLM-based methods exhibit notable limitations, particularly the lack of an effective adaptation mechanism for route length, which is critical for guiding retrosynthetic planning (Liu et al., 2023a).

To address these gaps, we propose RetroInText, a novel template-free retrosynthesis framework (as shown in Figure. 1). RetroInText incorporates ChatGPT to generate detailed reaction procedure descriptions, which include key information about the synthesis pathway, such as transition states, structural transformations, and energy barriers. These descriptions provide a textual representation of the reaction context, complementing molecular graph and 3D representations to enhance retrosynthesis prediction. In particular, we first use ChatGPT to obtain a description of the entire pathway, starting with the target product based on its name. This textual description, along with the molecular 3D geometry information is used as input information for training. For each selection step, we introduced multiple value functions, such as ScScore (Coley et al., 2018) and the text captioning score to rank candidate reactants. We employ an existing pre-trained MolT5 as our single-step approach to intermediate prediction. Therefore, RetroInText is a context-aware model that integrates molecular captioning and context embeddings. RetroInText utilizes contextual information from previous steps for the entire pathway, thereby enhancing retrosynthesis prediction accuracy.

We evaluated RetroInText on the RetroBench dataset constructed by Liu et al. (Liu et al., 2023a), they determined all possible synthetic routes for each target, resulting in a comprehensive set of routes for $128,469$ molecules. RetroBench dataset was constructed based on the USPTO-full dataset (Chen et al., 2020), which is a foundational resource for retrosynthetic planning. Extensive experimental results on retrosynthetic planning tasks demonstrate that RetroInText outperforms template-free baselines, achieving up to a 5% improvement in Top-1 test accuracy. Additionally, ablation experiments confirm the effectiveness of textual information and LLM. In brief, we highlight our main contributions as follows:

- We propose the RetroInText framework as a template-free approach to multi-step retrosynthesis prediction. When predicting subsequent steps in retrosynthesis, this framework integrates in-context textual information from previous steps.
- With RetroInText, we leverage the advantage of LLM and ChatGPT as our generative models and evaluate the reactions based on their molecular descriptions. A combination of textual information, molecular graphs, and 3D geometry information is used to select the optimal molecule in the selection phase.
- Extensive experiments have demonstrated that RetroInText achieves a competitive level of performance. Furthermore, RetroInText is tested in experiments to show its ability to predict complex reactions.

2 RELATED WORK

Single Step Retrosynthesis. Existing single-step retrosynthesis methods are categorized into template-based, semi-template-based, and template-free approaches. Template-based methods extract reaction templates from chemical reaction databases and model retrosynthesis as a classification or template retrieval task, mapping the product to reactants using predicted templates (Gaiński et al., 2024; Chen & Jung, 2021; Xie et al., 2023; Zhang et al., 2024a). Semi-template-based methods decompose the retrosynthesis problem into two steps. Including identifying reaction centers to generate synthons, and converting these synthons into reactants using generative models or adding leaving

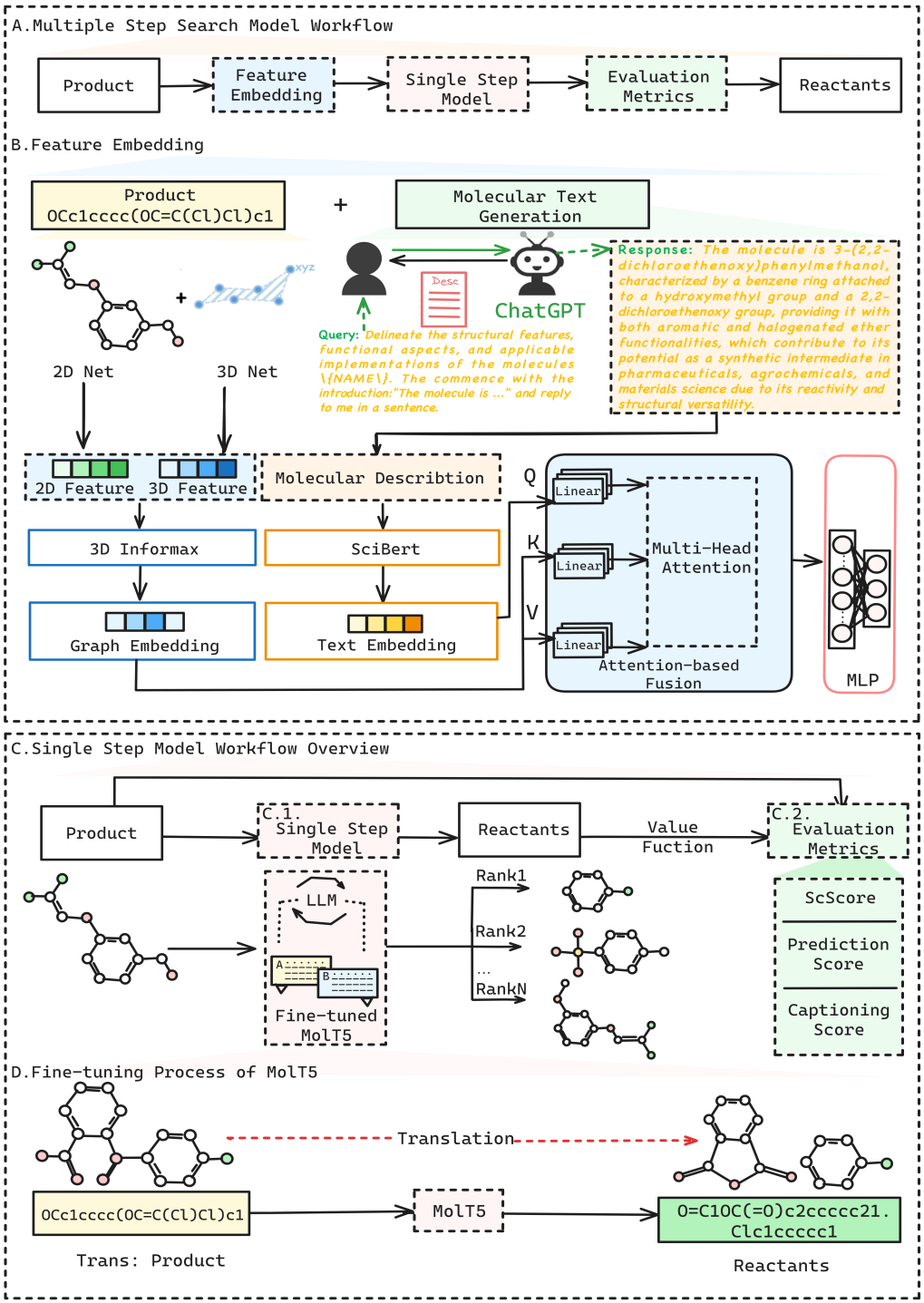

Figure 1: **Overview of the RetroInText. A** Multiple Step Search Model Workflow of RetroInText. **B** Feature Embedding. The product is represented as a molecular graph and 3D geometry features. It is combined with text embeddings generated by ChatGPT and processed through SciBERT for multimodal integration. **C** Single Step Model Workflow. **C.1** A fine-tuned MolT5 model generates potential reactants from the product, ranked by **C.2** Evaluation Metrics. Reactants are evaluated using ScScore, captioning score, and prediction score to determine synthetic routes' quality and feasibility. **D** MolT5 transforms the product SMILES into potential reactant structures.

groups (Zhong et al., 2023; Somnath et al., 2021; Zhu et al., 2023; Lan et al., 2024). Template-free methods treat retrosynthesis as either a sequence-to-sequence task using SMILES or a graph-editing task to modify atoms and bonds (Igashov et al., 2024; Andronov et al., 2024; Laabid et al., 2024; Yao et al., 2024; Liu et al., 2024d; Zhang et al., 2024b). With the development of multimodal LLMs, reasoning capabilities are being extended to retrosynthesis (M. Bran et al., 2024). Although textual information from LLM such as ChatGPT has been employed in single-step retrosynthesis models (Qian et al., 2023; Liu et al., 2024d), its integration into multi-step retrosynthesis processes remains unexplored (Christofidellis et al., 2023; Liu et al., 2023b).

Retrosynthesis Planning. Retrosynthesis Planning (RP) employs search algorithms to identify optimal candidates from single-step model predictions iteratively until all target compounds are sourced from existing commercial suppliers (Liu et al., 2023c; Zhao et al., 2023; Liu et al., 2024a; Zhang et al., 2024b; Zeng et al., 2024). These search algorithms can broadly be categorized into several types: Monte Carlo Tree Search (MCTS) employs a policy network to enhance retrosynthetic planning efficiency by effectively exploring and navigating the solution space (Segler et al., 2018). Retro* (Chen et al., 2020) proposed an AND-OR RP model using an A*-like heuristic, where OR nodes (reactions) require any child, and AND nodes (products) require all children. Modeling RP as an AND-OR tree has proven sound and effective. Recent works have focused on developing active frameworks (Torren-Peraire et al., 2024) and new evaluation methods (Tripp et al., 2024; Tian et al., 2024; Maziarz et al., 2024). For example, (Schreck et al., 2019) and (Liu et al.) assign a uniform cost of 1 to each reaction, optimizing for the shortest route. However, shorter routes may result in lower yields compared to longer routes. Consequently, (Liu et al., 2023a) proposed a novel multi-step planning approach based on a conventional search algorithm, but they lack an adaptation mechanism for route length and full-route information (Yuan et al., 2024). The aforementioned methodologies require the annotation of costs for every reaction step, and incorporating reliable reaction quality data from chemists or laboratory experimentation entails significant expenses. As a result, these approaches often become economically impractical.

3 PRELIMINARY

3.1 SINGLE-STEP RETROSYNTHESIS

Define the space of all molecules as $\mathcal{M}$. The single-step retrosynthesis aims to input a target molecule $T \in \mathcal{M}$, resulting in a prediction of the potential reactions and their related reactants as outcomes. We denote it as an injection:

$$O(\cdot): \quad T \rightarrow \{R_i, \mathcal{I}_i, c(R_i)\}_{i=1}^{k}, \tag{1}$$

where $O(\cdot)$ represents the single-step model, which outputs at most k reactions R_i with their following reactant sets $\mathcal{I}_i$ and costs $c(R_i)$. The costs can be the actual price of the reaction or just a negative log-likelihood of this reaction under the model.

3.2 RETROSYNTHETIC SCORING METHOD

The goal of retrosynthetic planning is to find a series of reactions that transform the starting material set $\mathcal{S} \subseteq \mathcal{M}$ to the target molecule $M_t \in \mathcal{M}$:

$$M_t \rightarrow I \rightarrow \mathcal{S}, \tag{2}$$

$I = \{m_1 \ldots, m_j\} \subseteq \mathcal{M} \setminus \mathcal{S}$ stands for the set of intermediate molecules. Beginning with the target molecule M_t, current strategies perform series single-step retrosynthesis predictions by model $O(\cdot)$ until all molecules at the leaf nodes are from $\mathcal{S}$, form pathways to synthesis M_t, which can be formulated as:

$$\mathcal{P} = \{p_1, p_2, ..., p_n\}, \tag{3}$$

where $\mathcal{P}$ represents the set of pathways to synthesis M_t.

4 METHODOLOGY

As shown in Figure. 1, our proposed framework RetroInText incorporates a pre-trained molecular representation model 3DInfomax (Stärk et al., 2022), which is utilized to embed both molecular

graph information and 3D structural data. We feature ChatGPT-3.5 for generating contextual textual information along the multi-step pathway. Additionally, we propose an attention-based mechanism that offers a fusion module to complement these multi-modal representations with in-context learning and a fine-tuned LLM MolT5 as a single-step retrosynthesis model.

4.1 Retrosynthesis Model

4.1.1 Single-step Model

We adopt MolT5 (Edwards et al., 2022) as our single-step model $O(\cdot)$. Specifically, MolT5 is a transformer-based model with an encoder-decoder architecture based on the T5 model, pre-trained on 100 million molecular SMILES as well as a C4 dataset which contains 700G textual data. The model is suited to generation tasks such as molecular captioning. It already contains a wealth of molecular and textual information. However, to adapt the model to our task, we apply a translation-based approach to fine-tune the model. Specifically, we extract all reactions from the training set and treat the products and reactants in SMILES as two distinct "languages" for translation. Details of fine-tuning MolT5 can be seen in Appendix A.3. In summary, we fine-tune MolT5 to accommodate retrosynthesis tasks (as shown in Figure. 1 D):

$$translation : products \rightarrow reactants, \tag{4}$$

where $products$ is the intermediate molecule during retrosynthetic planning, while the $reactants$ represent the corresponding reactant molecules. This approach equips the model with the capability to handle retrosynthesis tasks. We use it as our single-step model in the expansion phase to predict Top-k reactions and their corresponding reactants. The results of the single-step models can be seen in Appendix C.1.

4.1.2 Molecular Representation

Molecule Graph Encoder. We use 3DInfomax as the molecular graph and 3D encoder (Figure. 1B). The 3DInfomax model consists of a 2D GNN and a 3D GNN, utilizing a contrastive learning approach during training. It aligns the molecular graphs with the 3D conformations, maximizing the mutual information between the 2D GNN and the 3D conformation GNN, allowing the model to leverage both molecular structure and 3D conformation information simultaneously. We apply 3DInfomax during the selection process to fully utilize both molecular structure and 3D conformation information. The molecule is represented as a graph $\mathcal{G} = (\mathcal{V}, \mathcal{E})$, where $\mathcal{V}$ and $\mathcal{E}$ stands for the set of molecule nodes and edges respectively. RetroInText also includes information about the molecule's conformation as 3D cloud points $\{x_1, \cdots, x_m\} \subset \mathbb{R}^3$. Then we use 3DInfomax as the $M_Encoder$ of the graph to get the molecular model:

$$\boldsymbol{H}_m = M_Encoder(\mathcal{G}), \tag{5}$$

where $\boldsymbol{H}_m \in \mathbb{R}^d$, wherein d represents the output dimension of the model and the $\mathcal{G}$ corresponds to the graph representation of the intermediate molecules.

Textual Generator and Encoder. In this study, we utilize ChatGPT to generate text. Based on the IUPAC names of the products and intermediates, we create textual descriptions of the intermediate molecules along all pathways using ChatGPT. Chemical structures are uniquely represented by IUPAC names, which are derived from a set of rules mapping structures to linguistic phrases. Chemical structures described by IUPAC names are more natural and language-like than those described by SMILES. IUPAC names serve as a bridge between chemical molecules and LLMs. Details can be seen in Appendix B. We use the following prompts to generate textual descriptions:

> *Describe the key transition states involved in the synthesis of {{products}} from the intermediates {{intermediates}}. Explain the structural changes and energy barriers for each transition state, and reply to me in a sentence.*

where {{products}} corresponds to the IUPAC name of the product, and {{intermediates}} corresponds to the IUPAC names of all intermediate molecules. In cases with multiple intermediate molecules, they are concatenated using commas. When we obtain text information on the pathway to the target molecule $\mathcal{T} = \{t_1, t_2, \ldots, t_n\}$, SciBERT (Beltagy et al., 2019) is used as $T_Encoder$ for the textual modal (Figure. 1 B).

$$\boldsymbol{H}_t = T_Encoder(\mathcal{T}), \tag{6}$$

To ensure no information leakage and to eliminate variations in the textual content generated by ChatGPT during the test phase, we use only the structural information of the product molecules as the textual information for each step. This also ensures that the selected intermediates remain closely aligned with the product molecules. We generate textual descriptions using the following prompts:

> *Delineate the structural features, functional aspects, and applicable implementations of the molecules {NAME}. They commence with the introduction: "The molecule is ..." and reply to me in a sentence.*

where {NAME} corresponds to the IUPAC names of the products. SciBERT is also used as the encoder for textual information.

Multi-modal Fusion. While obtaining the molecular representations $\boldsymbol{H}_m$ and textual representations $\boldsymbol{H}_t$, we use an attention mechanism to fuse the two, treating the textual information as Q and the molecular representations as K and V:

$$\boldsymbol{Q} = \boldsymbol{H}_t \boldsymbol{W}^Q, \quad \boldsymbol{K} = \boldsymbol{H}_m \boldsymbol{W}^K, \quad \boldsymbol{V} = \boldsymbol{H}_m \boldsymbol{W}^V, \tag{7a}$$

$$Attention = \text{softmax}\left(\frac{\boldsymbol{Q}\boldsymbol{K}^T}{\sqrt{d_k}}\right)\boldsymbol{V}, \tag{7b}$$

$$\boldsymbol{H}_f = Attention(\boldsymbol{Q}, \boldsymbol{K}, \boldsymbol{V}), \tag{7c}$$

where $\boldsymbol{W}^Q \in \mathbb{R}^{d \times d_q}$,$\boldsymbol{W}^K \in \mathbb{R}^{d \times d_k}$ and $\boldsymbol{W}^V \in \mathbb{R}^{d \times d_v}$ are trainable parameters, $\boldsymbol{H}_f$ represents the fused representation (as shown in Figure. 1 B).

4.1.3 Model Training

We trained two different versions of the model: one is a scoring model to deal with the situation in which there is no textual information during the testing phase, and the other incorporates the fusion module into the model training process, which means $\boldsymbol{W}^Q$,$\boldsymbol{W}^K$ and $\boldsymbol{W}^V$ is incorporated into the model training. This allows the model to adapt to scenarios where textual information is present during testing:

$$\hat{\boldsymbol{y}} = MLP(\boldsymbol{H}_f), \tag{8}$$

$$L_{MSE} = \frac{1}{n}\sum_{i=1}^{n}(\boldsymbol{y}_i - \hat{\boldsymbol{y}}_i)^2, \tag{9}$$

where $\hat{\boldsymbol{y}}$ represents the model's prediction score, and the model is trained using the Mean Squared Error (MSE) loss.

4.2 Scoring Method for Guiding the Search

To guide the retrosynthesis search process, we employ a scoring framework that effectively ranks candidate pathways by combining synthetic complexity, reaction costs, and textual alignment. The scoring framework consists of three components: synthetic complexity score (ScScore), reaction cost score, and captioning score.

Synthetic Complexity and Reaction Cost Scores. The synthetic complexity score (ScScore), ranging from 1 to 5, quantifies molecular complexity while considering synthetic accessibility (Coley et al., 2018). For a retrosynthesis pathway, the synthetic complexity score V_t is defined in Equation 10a, where $\mathcal{I}_i$ denotes the i-th intermediate molecule, and n represents the total number of intermediates. This normalization ensures that lower scores correspond to simpler and more accessible intermediates.

The reaction cost score V_m, as defined in Equation 10b, evaluates the cumulative cost of reactions within the pathway, where $c(R_i)$ reflects the reaction cost for R_i, the reaction producing the intermediate molecule. This metric accounts for the feasibility and efficiency of the associated chemical transformations.

The overall pathway score V, defined in Equation 10c, combines the synthetic complexity and reaction cost scores, prioritizing pathways that are both synthetically accessible and cost-efficient.

$$V_t = \sum_{i=1}^{n}(1 - \frac{ScScore(\mathcal{I}_i) - 1}{4}), \tag{10a}$$

$$V_m = \sum_{i=1}^{n} c(R_i), \tag{10b}$$

$$V = V_t + V_m, \tag{10c}$$

Captioning Score for Pathway Reranking.

In addition to the core scoring components, we integrate the captioning score during the selection phase to enhance the selection process. The captioning score leverages textual descriptions generated during retrosynthesis planning to evaluate the alignment between the descriptions of intermediate molecules and the overall pathway context. This alignment provides an additional layer of interpretability and ensures the textual coherence of selected pathways.

During training, the synthetic complexity score, reaction cost score, and textual alignment are treated as true values, allowing the model to learn a unified scoring strategy. At inference, the combined scoring framework, including the captioning score, refines pathway ranking by ensuring both chemical feasibility and contextual consistency.

The inference process is summarized in Algorithm 1, where the scoring framework ranks pathways and guides molecule expansion. This integrated approach enables RetroInText to effectively identify retrosynthesis pathways that are optimal across multiple dimensions.

Algorithm 1 Retrosynthesis Planning Algorithm

```
Input: target molecule M_t, starting material set S, textual information T
Initialize: reactants set R = {}, path set P = {M_t}
while P is not empty do
    Take path p from P, predict reactants I_p for expansion given p by O(·)
    for reactant I_p^(i) in I_p do
        if I_p^(i) ∈ S then Put I_p^(i) into R
        else
            rank p' = p + [I_p^(i)] by computing captioning score of T
            put ranked p' into P
        end if
    end for
end while
return predicted reactant set R
```

5 EXPERIMENTS

5.1 EXPERIMENTAL SETUP

Dataset. We use the public dataset RetroBench (Liu et al., 2023a)(as shown in Table. 1) for evaluation, which includes $46,458$ molecules as the training set, $5,803$ molecules as the validation set and $5,838$ molecules as the Test set. The synthetic pathways for each molecule are extracted from the USTPO-full reaction network. All reactions along the pathways for each molecule in the training and validation set are extracted to fine-tune the MolT5 model.

Baselines. Retrosynthetic planning strategies integrate retrosynthesis models with search algorithms. We compare our model with template-based models, including Retrosim (Coley et al., 2017), Neuralsym (Segler & Waller, 2017), and GLN (Dai et al., 2019). We also compare with template-free models, such as Transformer (Karpov et al., 2019) Megan (Sacha et al., 2021) and FusionRetro (Liu et al., 2023a), as well as semi-template-based models, including G2Gs (Shi et al.,

#Molecules / Depth / Dataset	2	3	4	5	6	7	8	9	10	11	12	13
Training	22,903	12,004	5,849	3,268	1,432	594	276	107	25	0	0	0
Validation	2,862	1,500	731	408	179	74	34	13	2	0	0	0
Test	2,862	1,500	731	408	179	74	34	13	2	32	2	1

Table 1: Statistics of molecules at various depths summarized from the dataset.

2020) and GraphRetro (Somnath et al., 2021). Additionally, we compared RetroInText with FusionRetro+CREBM (Liu et al., 2024b) that incorporate energy functions for reranking. In detail, CREBM is a framework that enhances molecule synthesis by integrating energy functions to evaluate and rerank synthetic routes, thereby improving the quality of the generated pathways. Upon completion of the retrosynthesis training, we employ the first A*-like algorithm guided AND-OR tree search methods Retro* (Chen et al., 2020), Retro*-0, which is indeed a beam search algorithm, and Greedy DFS search algorithms.

Evaluation Metrics. We utilized the commonly employed evaluation performance metrics Top-k ($k = 1, 2, 3, 4, 5$) exact match accuracy to evaluate the retrosynthesis performance proposed by Liu et al. (2023a). The exact match accuracy is computed by comparing predicted reactants SMILES to the dataset's ground truth on the benchmark dataset. More experimental setups can be found in Appendix A.

5.2 RESULTS

Comparison with Baselines. The performance of all methods is presented in Table. 2. Compared with all template-free models and the reranked CREAM model and the SOTA model FusitonRetro (Liu et al., 2023a), our model RetroInText achieved the best performance, exceeding the Top-1 accuracy of FusionRetro with CREBM by 1.8%, achieving SOTA performance. RetroInText also demonstrated superior performance across different search algorithms, even approaching the top results of template-based methods with Retro*-0 and Greedy DFS, highlighting the benefits of using LLM and route description.

Search Algorithm / Single-step Models	Retro*					Retro*-0					Greedy DFS
	Top-1	Top-2	Top-3	Top-4	Top-5	Top-1	Top-2	Top-3	Top-4	Top-5	Top-1
Template-based											
Retrosim (Coley et al., 2017)	35.1	40.5	42.9	44.0	44.6	35.0	40.5	43.0	44.1	44.6	31.5
Neuralsym (Segler & Waller, 2017)	**41.7**	**49.2**	52.1	53.6	54.4	**42.0**	**49.3**	52.0	53.6	54.3	**39.2**
GLN (Dai et al., 2019)	39.6	48.9	**52.7**	**54.6**	**55.7**	39.5	48.7	**52.6**	**54.5**	**55.6**	38.0
Semi-template-based											
G2Gs (Shi et al., 2020)	5.4	8.3	9.9	10.9	11.7	4.2	6.5	7.6	8.3	8.9	3.8
GraphRetro (Somnath et al., 2021)	15.3	19.5	21.0	21.9	22.4	15.3	19.5	21.0	21.9	22.2	**14.4**
GraphRetro+CREBM (Liu et al., 2024b)	**16.3**	**20.1**	**21.6**	**22.3**	**22.7**	**16.3**	**20.2**	**21.6**	**22.3**	**22.7**	-
Template-free											
Transformer (Karpov et al., 2019)	31.3	40.4	44.7	47.2	48.9	31.2	40.5	45.1	47.3	48.7	26.7
Transformer+CREBM	35.0	43.4	46.7	48.7	49.7	34.0	43.1	46.4	48.3	49.4	-
Megan (Sacha et al., 2021)	18.8	27.9	32.7	36.6	38.1	18.6	27.7	32.6	36.4	38.5	32.9
FusionRetro (Liu et al., 2023a)	37.5	45.0	48.3	50.6	51.5	37.4	45.0	48.4	50.4	51.1	35.2
FusionRetro+CREBM (Liu et al., 2024b)	39.4	46.6	49.3	50.7	51.5	39.6	46.7	49.5	51.0	51.7	33.8
RetroInText (Ours)	**41.2**	**48.7**	**51.8**	**53.3**	**54.2**	**42.1**	**49.9**	**53.0**	**54.7**	**55.7**	**39.8**

Table 2: Summary of retrosynthetic planning results for exact match accuracy (%).

Analysis for the Depth of Routes. To better evaluate the performance of our proposed model across varying levels of retrosynthetic complexity, we analyzed the prediction accuracy at different depths using Greedy DFS, as shown in Figure. 2. Our model RetroInText demonstrates competitive performance across different depths, particularly excelling in longer synthesis routes. Compared to other baselines, our model maintains a more stable decline with increasing depth. While models

like GraphRetro and Megan sharply drop beyond depth 4, RetroInText retains a significant margin, demonstrating robustness and effectiveness in deeper, more complex retrosynthetic planning.

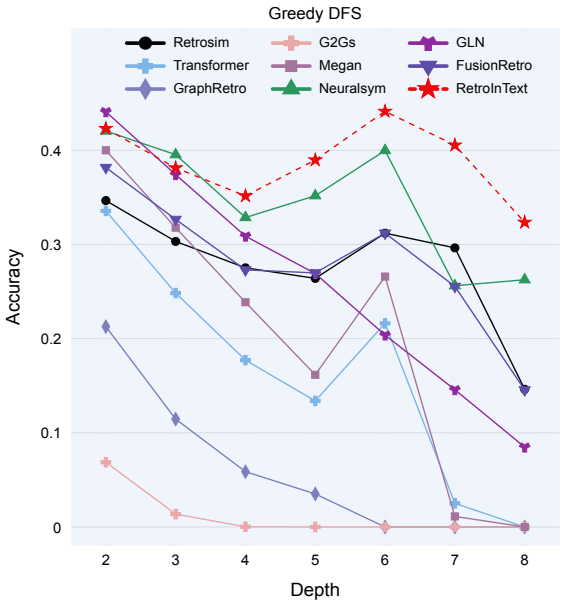

Figure 2: Test accuracy of retrosynthesis models combined with Greedy DFS at different depths. The red star stands for our method RetroInText.

Ablation Experiments. To better understand the contribution of each component within our proposed framework, we conducted a series of ablation experiments. As shown in Table. 3, our model RetroInText, consistently outperforms the baseline model across all Top-N accuracy metrics, demonstrating the effectiveness of our proposed enhancements. For instance, in terms of Top1 accuracy, RetroInText achieves a 4.0% increase over MolT5(SMILES). Similarly, compared to RetroInText(Graph), where we tested using FusionRetro (Liu et al., 2023a), which achieved 37.5%, RetroInText shows a 3.7% improvement. These results suggest that the synergy between structural features and text-aware components substantially enhances predictive accuracy. Additionally, the removal of the textual component, as indicated by the RetroInText (w/o text) configuration, results in a Top1 accuracy of 40.2%. Compared to the complete RetroInText model, which achieves 41.2%, highlighting the value of the textual module in providing essential contextual information that supports more accurate predictions. Further details on the analyses and experimental setup can be found in Appendix C, which provides additional insights into the significance of each module.

Additionally, we conducted experiments across different depths, which demonstrate that incorporating textual information consistently improves performance at all levels. As shown in Table. 4 Retro* outperforms Retro*(w/o text), particularly at increasing depths, showing robustness in predicting long synthetic routes. The most pronounced gains in Top-1 to Top-5 accuracy occur at deeper paths (Depths 5 to 8), highlighting the effectiveness of textual data in enhancing prediction accuracy for complex retrosynthetic planning tasks.

Methods	Top-1	Top-2	Top-3	Top-4	Top-5
RetroInText(SMILES)	35.6	41.6	44.1	45.4	46.2
MolT5 (SMILES)	37.2	43.7	46.2	47.4	48.3
RetroInText (Graph)	37.5	45.0	48.2	50.0	50.9
RetroInText (w/o text)	40.2	47.3	50.2	51.7	52.7
RetroInText (Ours)	**41.2**	**48.7**	**51.8**	**53.3**	**54.2**

Table 3: Ablation study of RetroInText for exact match accuracy (%).

Depth	Retro*(w/o text)					Retro*				
	Top-1	Top-2	Top-3	Top-4	Top-5	Top-1	Top-2	Top-3	Top-4	Top-5
Depth2	**45.0**	**52.4**	55.4	57.2	58.3	44.9	52.3	**55.4**	**57.3**	**58.3**
Depth3	38.9	45.9	49.3	50.5	51.5	**40.0**	**47.9**	**51.5**	**53.0**	**53.9**
Depth4	33.7	40.9	42.5	43.6	43.6	**36.1**	**43.6**	**46.4**	**47.7**	**48.3**
Depth5	35.5	41.7	43.4	44.4	44.4	**39.0**	**47.8**	**50.3**	**51.2**	**51.7**
Depth6	33.0	36.3	36.9	38.0	38.0	**36.3**	**40.8**	**41.9**	**43.0**	**44.1**
Depth7	25.7	31.1	31.1	31.1	31.1	**28.4**	**33.8**	**35.1**	**35.1**	**35.1**
Depth8	29.4	41.2	41.2	41.2	41.2	**32.4**	**41.2**	**44.1**	**47.1**	**47.1**

Table 4: Exact match accuracy (%) at different depths of ground truth synthetic routes.

6 CONCLUSIONS

In this work, we propose RetroInText, a novel framework for retrosynthetic planning that leverages contextual information along the synthetic route through ChatGPT. RetroInText employs in-context learning to incorporate textual information from previous steps, enhancing realistic retrosynthetic planning. Additionally, we used a fine-tuned LLM, MolT5 (Edwards et al., 2022), along with a pre-trained molecular representation model to integrate both molecular structure and 3D conformational data, improving the selection process. Experiments on the RetroBench dataset demonstrate that RetroInText outperforms existing template-free methods, achieving SOTA performance. Further experiments at various depths and ablation studies show the strength of text information during retrosynthetic planning. In the future, we are planning to develop an end-to-end question-answering model (Maziarz et al., 2022; Liu et al., 2023d) to further improve retrosynthetic step selection and enhance the utility of a deep learning-based retrosynthesis model.

REFERENCES

Mikhail Andronov, Natalia Andronova, Michael Wand, Djork-Arné Clevert, and Jürgen Schmidhuber. Accelerating the inference of string generation-based chemical reaction models for industrial applications. In *ICML'24 Workshop ML for Life and Material Science: From Theory to Industry Applications*, 2024.

Iz Beltagy, Kyle Lo, and Arman Cohan. SciBERT: A pretrained language model for scientific text. In Kentaro Inui, Jing Jiang, Vincent Ng, and Xiaojun Wan (eds.), *Proceedings of the 2019 Conference on Empirical Methods in Natural Language Processing and the 9th International Joint Conference on Natural Language Processing (EMNLP-IJCNLP)*, pp. 3615–3620, Hong Kong, China, November 2019. Association for Computational Linguistics.

Binghong Chen, Chengtao Li, Hanjun Dai, and Le Song. Retro*: learning retrosynthetic planning with neural guided a* search. In *International conference on machine learning*, pp. 1608–1616. PMLR, 2020.

Shuan Chen and Yousung Jung. Deep retrosynthetic reaction prediction using local reactivity and global attention. *JACS Au*, 1(10):1612–1620, 2021.

Dimitrios Christofidellis, Giorgio Giannone, Jannis Born, Ole Winther, Teodoro Laino, and Matteo Manica. Unifying molecular and textual representations via multi-task language modelling. In *International Conference on Machine Learning*, pp. 6140–6157. PMLR, 2023.

Connor W Coley, Luke Rogers, William H Green, and Klavs F Jensen. Computer-assisted retrosynthesis based on molecular similarity. *ACS central science*, 3(12):1237–1245, 2017.

Connor W Coley, Luke Rogers, William H Green, and Klavs F Jensen. Scscore: synthetic complexity learned from a reaction corpus. *Journal of chemical information and modeling*, 58(2): 252–261, 2018.

Hanjun Dai, Chengtao Li, Connor Coley, Bo Dai, and Le Song. Retrosynthesis prediction with conditional graph logic network. *Advances in Neural Information Processing Systems*, 32, 2019.

Carl Edwards, Tuan Lai, Kevin Ros, Garrett Honke, Kyunghyun Cho, and Heng Ji. Translation between molecules and natural language. pp. 375–413, 2022. Publisher Copyright: © 2022 Association for Computational Linguistics.; 2022 Conference on Empirical Methods in Natural Language Processing, EMNLP 2022 ; Conference date: 07-12-2022 Through 11-12-2022.

Piotr Gaiński, Michał Koziarski, Krzysztof Maziarz, Marwin Segler, Jacek Tabor, and Marek Śmieja. RetroGFN: Diverse and feasible retrosynthesis using GFlownets. In *ICLR 2024 Workshop on Generative and Experimental Perspectives for Biomolecular Design*, 2024.

Ilia Igashov, Arne Schneuing, Marwin Segler, Michael M. Bronstein, and Bruno Correia. Retrobridge: Modeling retrosynthesis with markov bridges. In *The Twelfth International Conference on Learning Representations*, 2024.

Pavel Karpov, Guillaume Godin, and Igor V Tetko. A transformer model for retrosynthesis. In *International Conference on Artificial Neural Networks*, pp. 817–830. Springer, 2019.

Junsu Kim, Sungsoo Ahn, Hankook Lee, and Jinwoo Shin. Self-improved retrosynthetic planning. In Marina Meila and Tong Zhang (eds.), *Proceedings of the 38th International Conference on Machine Learning*, volume 139 of *Proceedings of Machine Learning Research*, pp. 5486–5495. PMLR, 18–24 Jul 2021.

Najwa Laabid, Severi Rissanen, Markus Heinonen, Arno Solin, and Vikas Garg. Aligned diffusion models for retrosynthesis. In *ICML 2024 Workshop on Structured Probabilistic Inference & Generative Modeling*, 2024.

Zixun Lan, Binjie Hong, Jiajun Zhu, Zuo Zeng, Zhenfu Liu, Limin Yu, and Fei Ma. Retrosynthesis prediction via search in (hyper) graph, 2024.

G Liu, D Xue, S Xie, Y Xia, A Tripp, K Maziarz, M Segler, T Qin, Z Zhang, and TY Liu. Retrosynthetic planning with dual value networks, 2023.

Pengfei Liu, Yiming Ren, Jun Tao, and Zhixiang Ren. Git-mol: A multi-modal large language model for molecular science with graph, image, and text. *Computers in biology and medicine*, 171:108073, 2024a.

Songtao Liu, Zhengkai Tu, Minkai Xu, Zuobai Zhang, Lu Lin, Rex Ying, Jian Tang, Peilin Zhao, and Dinghao Wu. Fusionretro: molecule representation fusion via in-context learning for retrosynthetic planning. In *International Conference on Machine Learning*, pp. 22028–22041. PMLR, 2023a.

Songtao Liu, Hanjun Dai, Yue Zhao, and Peng Liu. Preference optimization for molecule synthesis with conditional residual energy-based models. In *Forty-first International Conference on Machine Learning*, 2024b.

Xiaoyi Liu, Hongpeng Yang, Chengwei Ai, Yijie Ding, Fei Guo, and Jijun Tang. Mvml-mpi: Multi-view multi-label learning for metabolic pathway inference. *Briefings in Bioinformatics*, 24(6): bbad393, 2023b.

Xiaoyi Liu, Chengwei Ai, Hongpeng Yang, Ruihan Dong, Jijun Tang, Shuangjia Zheng, and Fei Guo. Retrocaptioner: beyond attention in end-to-end retrosynthesis transformer via contrastively captioned learnable graph representation. *Bioinformatics*, 40(9):btae561, 2024c.

Yifeng Liu, Hanwen Xu, Tangqi Fang, Haocheng Xi, Zixuan Liu, Sheng Zhang, Hoifung Poon, and Sheng Wang. T-rex: Text-assisted retrosynthesis prediction, 2024d.

Zequn Liu, Wei Zhang, Yingce Xia, Lijun Wu, Shufang Xie, Tao Qin, Ming Zhang, and Tie-Yan Liu. MolXPT: Wrapping molecules with text for generative pre-training. In Anna Rogers, Jordan Boyd-Graber, and Naoaki Okazaki (eds.), *Proceedings of the 61st Annual Meeting of the Association for Computational Linguistics (Volume 2: Short Papers)*, pp. 1606–1616, Toronto, Canada, July 2023c. Association for Computational Linguistics.

Zhiyuan Liu, Sihang Li, Yanchen Luo, Hao Fei, Yixin Cao, Kenji Kawaguchi, Xiang Wang, and Tat-Seng Chua. MolCA: Molecular graph-language modeling with cross-modal projector and uni-modal adapter. In Houda Bouamor, Juan Pino, and Kalika Bali (eds.), *Proceedings of the 2023 Conference on Empirical Methods in Natural Language Processing*, pp. 15623–15638, Singapore, December 2023d. Association for Computational Linguistics.

Andres M. Bran, Sam Cox, Oliver Schilter, Carlo Baldassari, Andrew D White, and Philippe Schwaller. Augmenting large language models with chemistry tools. *Nature Machine Intelligence*, pp. 1–11, 2024.

Krzysztof Maziarz, Henry Richard Jackson-Flux, Pashmina Cameron, Finton Sirockin, Nadine Schneider, Nikolaus Stiefl, Marwin Segler, and Marc Brockschmidt. Learning to extend molecular scaffolds with structural motifs. In *International Conference on Learning Representations*, 2022.

Krzysztof Maziarz, Austin Tripp, Guoqing Liu, Megan Stanley, Shufang Xie, Piotr Gaiński, Philipp Seidl, and Marwin Segler. Re-evaluating retrosynthesis algorithms with syntheseus. In *ICLR 2024 Workshop on Generative and Experimental Perspectives for Biomolecular Design*, 2024.

Stephen Obonyo, Nicolas Jouandeau, and Dickson Owuor. Retrog: Retrosynthetic planning with tree search and graph learning. In *ICLR 2023-Machine Learning for Drug Discovery workshop*, 2023.

Adam Paszke, Sam Gross, Francisco Massa, Adam Lerer, James Bradbury, Gregory Chanan, Trevor Killeen, Zeming Lin, Natalia Gimelshein, Luca Antiga, Alban Desmaison, Andreas Kopf, Edward Yang, Zachary DeVito, Martin Raison, Alykhan Tejani, Sasank Chilamkurthy, Benoit Steiner, Lu Fang, Junjie Bai, and Soumith Chintala. Pytorch: An imperative style, high-performance deep learning library. In H. Wallach, H. Larochelle, A. Beygelzimer, F. d'Alché-Buc, E. Fox, and R. Garnett (eds.), *Advances in Neural Information Processing Systems*, volume 32. Curran Associates, Inc., 2019.

Yujie Qian, Zhening Li, Zhengkai Tu, Connor Coley, and Regina Barzilay. Predictive chemistry augmented with text retrieval. In Houda Bouamor, Juan Pino, and Kalika Bali (eds.), *Proceedings of the 2023 Conference on Empirical Methods in Natural Language Processing*, pp. 12731–12745, Singapore, December 2023. Association for Computational Linguistics.

Mikołaj Sacha, Mikołaj Błaz, Piotr Byrski, Paweł Dabrowski-Tumanski, Mikołaj Chrominski, Rafał Loska, Paweł Włodarczyk-Pruszynski, and Stanisław Jastrzebski. Molecule edit graph attention network: modeling chemical reactions as sequences of graph edits. *Journal of Chemical Information and Modeling*, 61(7):3273–3284, 2021.

John S Schreck, Connor W Coley, and Kyle JM Bishop. Learning retrosynthetic planning through simulated experience. *ACS central science*, 5(6):970–981, 2019.

Marwin HS Segler and Mark P Waller. Neural-symbolic machine learning for retrosynthesis and reaction prediction. *Chemistry–A European Journal*, 23(25):5966–5971, 2017.

Marwin HS Segler, Mike Preuss, and Mark P Waller. Planning chemical syntheses with deep neural networks and symbolic ai. *Nature*, 555(7698):604–610, 2018.

Chence Shi, Minkai Xu, Hongyu Guo, Ming Zhang, and Jian Tang. A graph to graphs framework for retrosynthesis prediction. In *International conference on machine learning*, pp. 8818–8827. PMLR, 2020.

Vignesh Ram Somnath, Charlotte Bunne, Connor Coley, Andreas Krause, and Regina Barzilay. Learning graph models for retrosynthesis prediction. *Advances in Neural Information Processing Systems*, 34:9405–9415, 2021.

Hannes Stärk, Dominique Beaini, Gabriele Corso, Prudencio Tossou, Christian Dallago, Stephan Günnemann, and Pietro Liò. 3d infomax improves gnns for molecular property prediction. In *International Conference on Machine Learning*, pp. 20479–20502. PMLR, 2022.

Sara Szymkuć, Ewa P Gajewska, Tomasz Klucznik, Karol Molga, Piotr Dittwald, Michał Startek, Michał Bajczyk, and Bartosz A Grzybowski. Computer-assisted synthetic planning: the end of the beginning. *Angewandte Chemie International Edition*, 55(20):5904–5937, 2016.

Chengyang Tian, Yangpeng Zhang, and Yang Liu. Retro-prob: Retrosynthetic planning based on a probabilistic model, 2024.

Paula Torren-Peraire, Jonas Verhoeven, Dorota Herman, Hugo Ceulemans, Igor V. Tetko, and Jörg K. Wegner. Improving route development using convergent retrosynthesis planning. In *ICML'24 Workshop ML for Life and Material Science: From Theory to Industry Applications*, 2024.

Austin Tripp, Krzysztof Maziarz, Sarah Lewis, Marwin Segler, and José Miguel Hernández-Lobato. Retro-fallback: retrosynthetic planning in an uncertain world. In *The Twelfth International Conference on Learning Representations*, 2024.

Jiancong Xie, Yi Wang, Jiahua Rao, Shuangjia Zheng, and Yuedong Yang. Self-supervised contrastive molecular representation learning with a chemical synthesis knowledge graph. *Journal of Chemical Information and Modeling*, 64(6):1945–1954, 2024.

Shufang Xie, Rui Yan, Junliang Guo, Yingce Xia, Lijun Wu, and Tao Qin. Retrosynthesis prediction with local template retrieval. In *Proceedings of the AAAI Conference on Artificial Intelligence*, volume 37, pp. 5330–5338, 2023.

Lin Yao, Wentao Guo, Zhen Wang, Shang Xiang, Wentan Liu, and Guolin Ke. Node-aligned graph-to-graph: Elevating template-free deep learning approaches in single-step retrosynthesis. *JACS Au*, 4(3):992–1003, February 2024. ISSN 2691-3704.

Chengxuan Ying, Tianle Cai, Shengjie Luo, Shuxin Zheng, Guolin Ke, Di He, Yanming Shen, and Tie-Yan Liu. Do transformers really perform badly for graph representation? In M. Ranzato, A. Beygelzimer, Y. Dauphin, P.S. Liang, and J. Wortman Vaughan (eds.), *Advances in Neural Information Processing Systems*, volume 34, pp. 28877–28888. Curran Associates, Inc., 2021.

Yemin Yu, Ying Wei, Kun Kuang, Zhengxing Huang, Huaxiu Yao, and Fei Wu. Grasp: Navigating retrosynthetic planning with goal-driven policy. In S. Koyejo, S. Mohamed, A. Agarwal, D. Belgrave, K. Cho, and A. Oh (eds.), *Advances in Neural Information Processing Systems*, volume 35, pp. 10257–10268. Curran Associates, Inc., 2022.

Luotian Yuan, Yemin Yu, Ying Wei, Yongwei Wang, Zhihua Wang, and Fei Wu. Active retrosynthetic planning aware of route quality. In *The Twelfth International Conference on Learning Representations*, 2024.

Tao Zeng, Zhehao Jin, Shuangjia Zheng, Tao Yu, and Ruibo Wu. Developing bionavi for hybrid retrosynthesis planning. *JACS Au*, 4(7):2492–2502, 2024.

Qiang Zhang, Juan Liu, Wen Zhang, Feng Yang, Zhihui Yang, and Xiaolei Zhang. A multi-stream network for retrosynthesis prediction. *Frontiers of Computer Science*, 18(2):182906, 2024a.

Xu Zhang, Yiming Mo, Wenguan Wang, and Yi Yang. Retrosynthesis prediction enhanced by in-silico reaction data augmentation, 2024b.

Haiteng Zhao, Shengchao Liu, Ma Chang, Hannan Xu, Jie Fu, Zhihong Deng, Lingpeng Kong, and Qi Liu. Gimlet: A unified graph-text model for instruction-based molecule zero-shot learning. *Advances in Neural Information Processing Systems*, 36:5850–5887, 2023.

Shuangjia Zheng, Tao Zeng, Chengtao Li, Binghong Chen, Connor W Coley, Yuedong Yang, and Ruibo Wu. Deep learning driven biosynthetic pathways navigation for natural products with bionavi-np. *Nature Communications*, 13(1):3342, 2022.

Weihe Zhong, Ziduo Yang, and Calvin Yu-Chian Chen. Retrosynthesis prediction using an end-to-end graph generative architecture for molecular graph editing. *Nature Communications*, 14(1): 3009, 2023.

Jiajun Zhu, Binjie Hong, Zixun Lan, and Fei Ma. Single-step retrosynthesis via reaction center and leaving groups prediction. In *2023 16th International Congress on Image and Signal Processing, BioMedical Engineering and Informatics (CISP-BMEI)*, pp. 1–5. IEEE, 2023.

A EXPERIMENTAL PROCEDURE AND SETUP

A.1 EVALUATION METRIC

The current search algorithms (Segler et al., 2018; Chen et al., 2020; Kim et al., 2021; Yu et al., 2022; Obonyo et al., 2023; Yuan et al., 2024; Xie et al., 2024) mainly use search success rate as an evaluation metric, without verifying whether the identified materials can indeed synthesize target molecules. When combining existing one-step models, which achieve top-k accuracies in the range of 60% to 80%, with the Retro* algorithm, we observe that the search success rates for the overall multi-step retrosynthesis process reach between 85% and 94% (Figure. 3)(Liu et al., 2023a). This result is counterintuitive, as one would expect the success rate to decrease with each additional synthesis step. Therefore, we use the new evaluation metric proposed by FusionRetro (Liu et al., 2023a): the set of precise matches between the suggested actual material and the baseline truth. That is, it is correct when the set of actual materials obtained from the model is consistent with at least one of the possible multiple synthesis paths in the target molecule test set, and paper cuttings search is also conducted. When the length of the predicted synthesis path exceeds the depth of the real synthesis path, the search is stopped. We use the starting materials obtained from the reaction network in RetroBench as the base facts and compare them with the starting materials identified through the search process.

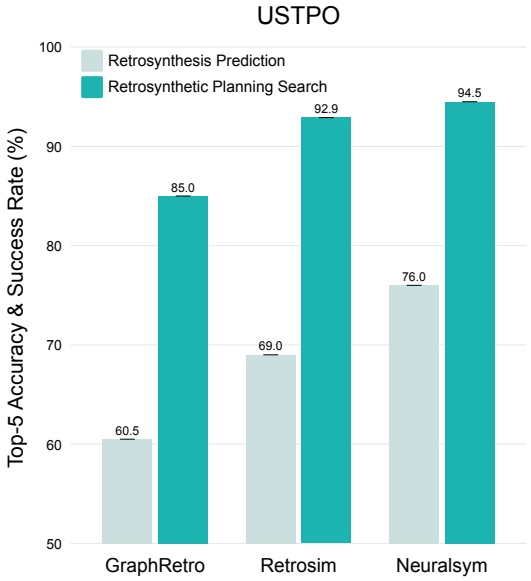

Figure 3: Performance of different retrosynthesis model for retrosynthesis prediction and multi-step planning on USPTO dataset.

A.2 IMPLEMENTATION DETAILS

We use Pytorch (Paszke et al., 2019) to implement our models. The codes of all baselines are implemented referring to the implementations of FusionRetro (Liu et al., 2023a) and CREBM (Liu et al., 2024b) . All the experiments of baselines are conducted on a single NVIDIA 4090 with 24GB memory size. The softwares that we use for experiments are Python 3.8.19, CUDA 11.5.119, einops 0.7.0, pytorch 2.2.0, pytorch-scatter 2.1.2, pytorch-sparse 0.6.18, numpy 1.24.4, torchvision 0.17.0. The total inference time is 79.5 hours.

A.3 FINE-TUNE PROCESS

All reaction in the training set is extracted as the fine-tuned dataset which includes more than $150K$ reactions. We trained it for 40 epochs, and chose the best checkpoint as a single-step model. The detailed training parameters are shown in Table. 5.

Parameter	Value	Description
Learning rate	$5 \cdot 10^{-5}$	Step size for optimization
Batch size	8	Number of samples per batch
Epochs	40	Number of training iterations
Hidden layers	24	Number of layers in the model
Hidden units	768	Number of neurons per layer
Head number	12	Number of multi-head per layer
Save steps	5000	Save checkpoint step
Beam number	4	Beam search number
Weight decay	0.1	Regularization coefficient

Table 5: Fine-tune parameters.

B MOLECULE NAME GENERATION

Before using ChatGPT to generate the text information for the routes, we should get the IUPAC names as mentioned in Section 4.1.2. Specifically, we extracted all the intermediates with the matched depth in the training set for all products then generated products and corresponding intermediate names. For the test set, we generated the IUPAC names of the products, but we only need them during creation. PubChemPy generates IUPAC names for all molecules.

C MORE RESULTS

C.1 SINGLE-STEP MODEL RESULTS

All the reactions in the test dataset are extracted for evaluating single-step models, with an overall $24,972$ reactions. The results are shown in Table. 6

Models	Top-k accuracy (%)			
	Top-1	Top-3	Top-5	Top-10
FusionRetro	31.1	39.4	**42.3**	**47.0**
Transformer	28.1	38.7	41.8	46.0
MolT5-small	20.8	30.0	33.9	38.3
MolT5-base(Ours)	**33.3**	**39.9**	42.1	44.5

Table 6: Retrosynthesis prediction results for exact match accuracy (%)

C.2 PROMPT IMPACT ON PATHWAY DESCRIPTIONS

To test the impact of text quality on the model, Specifically, two distinct prompts were evaluated, as outlined in Table. 7, to assess their impact on the textual descriptions of the molecule O=C1N=C(O)CN1N=C(O)C=Cc1ccc(Cl)c(C(F)(F)F)c1.The first prompt was designed to generate detailed, yet excessively verbose descriptions, while the second prompt focused on producing concise and targeted textual outputs.

Prompt1 was characterized by a lack of specificity, resulting in verbose descriptions with considerable redundancy. These excessive details, which included irrelevant information, had a detrimental effect on the model's accuracy. In contrast, Prompt 2 was deliberately designed to prioritize

clarity and relevance, avoiding superfluous content. The generated text was both concise and well-structured, contributing to an enhancement in downstream model performance.As illustrated in Table. 8, the use of text generated from the higher-quality prompt led to a notable improvement in the performance of the framework. Specifically, the Top-1 accuracy increased from 39.2% to 41.2%, while the Top-5 accuracy improved from 46.9% to 54.2%. These results underscore the significance of carefully crafting prompts to generate concise, high-quality text in order to achieve better model predictions.

Target Molecule	Prompt	Text
O=C1N=C(O)CN1N=C(O)C=Cc1ccc(Cl)c(C(F)(F)F)c1	Please describe the structural features, functional aspects, and applicable implementation methods of the molecule product, and describe the potential intermediate molecules intermediates in the synthesis pathway, with each intermediate molecule separated by "[SEP]". Additionally, provide a different reaction pathway and describe it.	The molecule 3-[4-chloro-3-(trifluoromethyl)phenyl]-N-(2,4-dioxoimidazolidin-1-yl)prop-2-enamide is a complex organic compound that features a substituted phenyl group, an imidazolidin-1-yl moiety, and a prop-2-enamide functional group.
O=C1N=C(O)CN1N=C(O)C=Cc1ccc(Cl)c(C(F)(F)F)c1	Describe the key transition states involved in the synthesis of products from the intermediates intermediates. Explain the structural changes and energy barriers for each transition state, and reply to me in a sentence.	The key transition states involved in the synthesis include the formation of an imine intermediate through the condensation of the prop-2-enoic acid and the amine group, followed by the cyclization of the imine to form the imidazolidin-1-yl ring.

Table 7: Comparison of Prompts and Textual Descriptions

Model	Top-1	Top-2	Top-3	Top-4	Top-5
RetroInText (prompt1)	39.2	43.4	45.6	45.7	46.9
RetroInText (prompt2)	41.2	48.7	51.2	53.3	54.2

Table 8: Comparison of prompt influence on textual quality for molecular descriptions and reactions

Target Molecule	Text (ChatGPT-3.5)	Text (ChatGPT-4)	Similarity
CC(C)Nc1ncnc2cscc12	There are two key transition states involved in the synthesis: the conversion of 2-chloro-N-propan-2-ylthieno[3,4-d]pyrimidin-4-amine to N-propan-2-ylthieno[3,4-d]pyrimidin-4-amine, with the structural change being the displacement of the chlorine atom by the amine group, and the conversion of N-propan-2-ylthieno[3,4-d]pyrimidin-4-amine to N-propan-2-ylthieno[3,4-d]pyrimidin-4-amine, with the structural change being the formation of the final amine functionality; both transitions have energy barriers that must be overcome for the reactions to proceed.	The key transition states involved in the synthesis of N-propan-2-ylthieno[3,4-d]pyrimidin-4-amine from 2-chloro-N-propan-2-ylthieno[3,4-d]pyrimidin-4-amine include a nucleophilic substitution, where the chlorine atom is replaced by an amine group, and a tautomeric shift, where the newly added amine group rearranges to a more stable position on the pyrimidine ring; both transition states involve overcoming energy barriers associated with breaking and forming chemical bonds and achieving the most stable and low energy conformation of the molecule.	These texts by different models describe the same key transition states, including the nucleophilic substitution where the chlorine atom is replaced by an amine group, and a tautomeric shift. Both mention energy barriers involved in the transition states.
CN=C(O)NCCNCc1cc[nH]n1	The key transition states involved in the synthesis of 1-methyl-3-[2-(1H-pyrazol-5-ylmethylamino)ethyl]urea from the intermediates N'-(1H-pyrazol-5-ylmethyl)ethane-1,2-diamine include the formation of a urea linkage and the addition of a methyl group. These transitions involve structural rearrangements and energy barriers that facilitate the conversion of the intermediates into the desired product.	The key transition states involved in the synthesis of 1-methyl-3-[2-(1H-pyrazol-5-ylmethylamino)ethyl]urea from N'-(1H-pyrazol-5-ylmethyl)ethane-1,2-diamine include the formation of an isourea intermediate followed by a rearrangement to the final urea product, each with associated energy barriers due to the breaking and forming of bonds and the structural changes from a linear to a more complex, cyclic arrangement.	The mechanisms and transformations described in both are similar, involving the formation of the urea bond and methylation.

Table 9: Comparison of textual descriptions generated by ChatGPT-3.5 and ChatGPT-4

C.3 Comparison of Outputs between GPT-3.5 and GPT-4

We employed GPT-4 for text generation, and a comparison between the outputs generated by GPT-4 and GPT-3.5 revealed a high degree of similarity in both content and the structural transformations described, as illustrated by the examples provided in Table. 9. Specifically, both models effectively characterized key transition states for the target molecules, including nucleophilic substitutions, tautomeric shifts, and the associated energy barriers for bond-breaking and bond-forming processes.

However, GPT-4 presented certain practical challenges, particularly with frequent API key limitations, which disrupted the workflow and diminished its reliability for consistent use. In contrast, GPT-3.5 exhibited stable performance without such restrictions, making it a more dependable choice for our framework. Given the negligible differences in performance and the operational constraints of GPT-4, GPT-3.5 was selected as the primary text generator for the experiments.

C.4 Ablation Study

To test the role of each part in the framework, we perform the ablation study on RetroInText. First, we used the no fine-tuning MolT5 model as the single-step model and observed that the generated SMILES strings for the corresponding molecules were invalid, resulting in scores of 0 across all cases. This indicates that the original MolT5 model is not suitable for our task, and fine-tuning is necessary. We also conducted the experiment only using the combination of SMILES and text to train the model, however, this combination is inferior to those of a multimodal approach. Next, we used the fine-tuned MolT5 as the single-step model, without incorporating the molecular representation model or textual information, and only relied on molecule fingerprints for scoring. Finally, we introduced textual information into the training process and used 3DInfomax as the molecular representation model, while excluding textual information during testing. The results demonstrate a significant improvement in multi-step accuracy when textual context information is included, indicating that using textual information in multi-step processes is highly effective. The case of depth3 (Figure. 4) shows text can make accurate predictions compared to not using text.

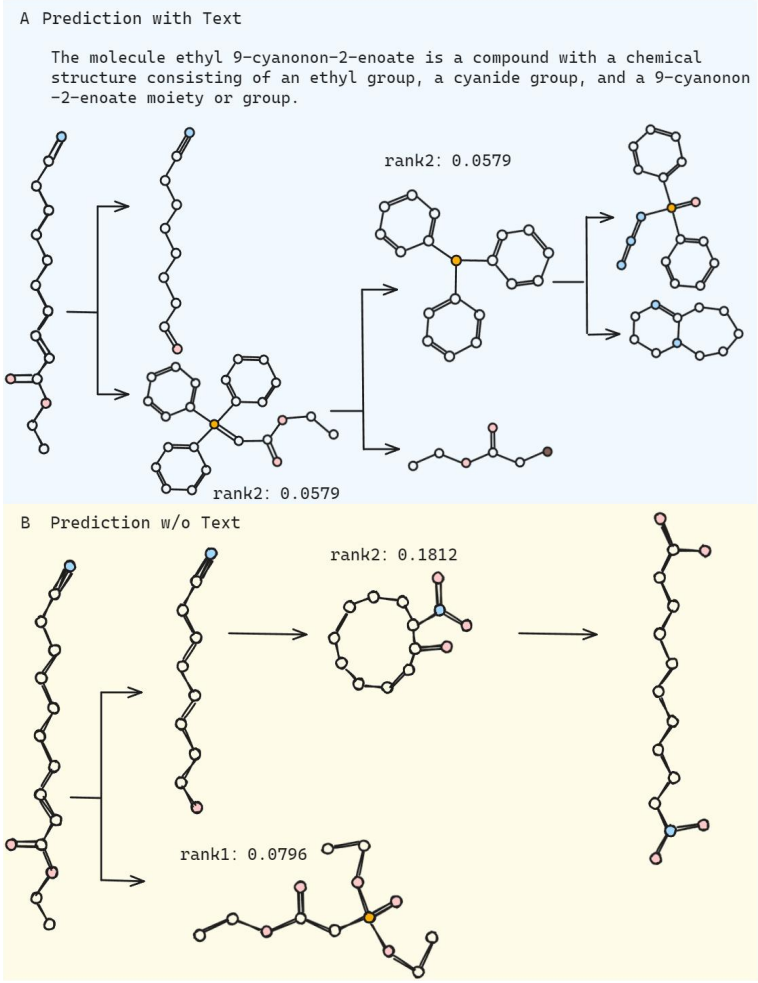

Figure 4: Comparison of retrosynthesis prediction with text (**A**) and without text (**B**)